ISSN: 2710-0588

Molecular Dynamics Simulation of Methane Adsorption and Diffusion

Jie Xiang[1], Guoqi Dong[2,*], and Jiandong Li[3]

[1] Inner Mongolia seventh geological mineral exploration and development limited liability company, HoHhot 010020, China

[2] China University of Mining and Technology (Beijing), Beijing 100083, China

[3] College of Resource and Environmental Sciences, Hebei Minzu Normal University for Nationalities, Chengde 067000, China

[*]Corresponding Author

Abstract

To study the adsorption and diffusion mechanism of low-rank coal at the microscopic level, samples of Fukang low-rank coal were collected, and the elemental composition, carbon type distribution and functional group type of the Fukang low-rank coal structure were determined by elemental analysis (Ea), Fourier-transform interferometric radiometer (FTIR), X-ray photoelectron spectroscopy (XPS) and ^{13}C nuclear magnetic resonance (^{13}C NMR) experiments to construct a 2D molecular structure of the coal and a 3D macromolecular structure model. The adsorption and diffusion characteristics of methane were researched by giant regular Monte Carlo (GCMC) and molecular dynamics (MD) simulation methods. The results showed that the excess adsorption amount of methane increased and then decreased with the increase in pressure. The diffusion of methane showed two stages with increasing pressure: a sharp decrease in the diffusion coefficient from 0.5 to 5.0 MPa and a slow decrease in the diffusion coefficient from 5.0 to 15.0 MPa. The lower the pressure, the larger the effective radius of the CH_4 and C atoms, and the higher the temperature, the more pronounced the diffusion and the larger the effective radius.

Keywords

List the; Low-rank Coal; Molecular Structure; Adsorption; Diffusion; Molecular Dynamics.

1. Introduction

Molecular simulation is widely used to construct the molecular structure of coal and study the mechanism of coal and methane interaction at the microscopic level [11]. To optimize gas production from coal reservoir rocks, an understanding of diffusion kinetics is a prerequisite [2]. The gas diffusion in the coal matrix is a vital process for mass migration from the pores to the cleats [10]. Molecular dynamics simulation is one of the most effective methods to study the microscopic mechanism of adsorbent diffusion [1].

The methane in the coal reservoir is mainly in the adsorbed state and the free state, which can be transformed into each other. As the pore pressure decreases, the methane adsorbed on the coal surface is desorbed, the adsorbed gas is converted into free gas and the gas diffuses from the coal matrix into the cleat system, from where it infiltrates the production well. Previous studies have concluded that coal particles, pores, temperature, pressure and water are the main factors affecting the adsorption and diffusion of methane in coal [3]. By comparing the adsorption and diffusion of methane, N_2 and CO_2, the loading amounts in pore models increased with increasing pore size, and the larger pores were more conducive to gas diffusion [4]. As the

ISSN: 2710-0588

pore size decreases, the self-diffusion coefficient also decreases, and in smaller pores, the molecular motion is weakened overall [5]. In different pores, the magnitude of the transport diffusion coefficient at low pressure is opposite to that at high pressure [6]. Gases have three diffusion coefficients: the self-diffusion coefficient, modified diffusion coefficient and migrating diffusion coefficient. All three different diffusion coefficients increased with increasing temperature, and the transport diffusion coefficient increased and then decreased with increasing pressure, reaching a peak [7]. Temperature and pressure significantly affect the diffusion of gases, where the increase in temperature is beneficial to the diffusion of gas, and the rise in pressure makes the diffusion coefficient increase first and then decrease, reaching the peak value (3.0 MPa) [9]. The increase in moisture within the pore space reduces the sorption properties, and internal moisture is negatively correlated with the self-diffusion and transport diffusion coefficients [8]. Water molecules interfere with the sorption and diffusion of CO_2 and CH_4 [9]. The diffusion coefficient decreases with increasing particle size and increases with increasing pressure and temperature [10]. The diffusion of CH_4 in shales is related to the sorbent's concentration, and the effective diffusion coefficient increases with increasing pressure and decreases with increasing temperature [11]. The diffusion coefficient in hard coals decreases with increasing grain size, while in brittle coals, the diffusion coefficient varies randomly within a small range of values with increasing grain size [12]. The larger the particle size, the slower the initial gas diffusion rate and the longer the time required to reach the desorption equilibrium. The higher the adsorption pressure, the greater the initial gas diffusion rate and the greater the accumulation of diffused gas [13]. Although a large number of previous studies on CH_4 diffusion in coal have been carried out at the molecular level, no one has yet used SWNTs to model the adsorption and diffusion of CH_4 by drilling cylindrical pores of different pore sizes in a macromolecular model of coal.

2. Materials and Methods

2.1. Molecular Structure Construction

2.1.1. Proximate Analysis and Ultimate Analysis

We tested the samples for organic elements using Elementar vario el III (Vario EL Ⅲ, Elementar, Hanau, Germany), and the test mode was CHNS mode / O mode.

2.1.2. FTIR Spectroscopy

Spectral analysis can be used to determine the presence of compounds or functional groups in the sample. The absorption peaks of the infrared spectrum of coal can be divided into four types: (1) the absorption peaks of coal at 700 ~ 900 cm^{-1} are an aromatic structure; (2) the absorption peaks of coal at 1000 ~ 1800 cm^{-1} are an oxygen-containing functional group; (3) the range from 2800 to 3000 cm^{-1} is the stretching vibration absorption band of aliphatic hydrocarbon CH_x; and (4) the hydroxyl group has an absorption peak between 3000 and 3600 cm^{-1} [13].

2.1.3. XPS Experimen

XPS is an experimental tool for quantifying information about the different chemical functional groups in the structure of coal and is often used to characterize the chemical structure of organic matter [8]. The instrument used for the X-ray photoelectron spectroscopy (XPS) experiments was Thermo Scientific K-Alpha (XPS, Thermo Fisher Scientific, Waltham, America).

2.1.4. ^{13}C NMR Measurement

^{13}C NMR has been shown to verify the chemical shifts of functional groups in the structure of coal, with different functional groups having different chemical shifts [5]. The solid-state dipolar decoupling magic angle spinning (DD/MAS) ^{13}C nuclear magnetic resonance (^{13}C NMR) measurement was performed using the JNM-ECZ600R spectrometer manufactured by JEOL Company (Shoshima City, Tokyo, Japan).

ISSN: 2710-0588

2.1.5. Molecular Structure Construction

Construction of the chemical structure of Fukang coal has been based mainly on experimental results from ^{13}C NMR and XPS measurements. FTIR spectroscopy has also been used to verify certain chemical functional groups such as –C=O, –OH, $–CH_2$ and $-CH_3$ [14]. XPS analysis data allow estimation of the relative content of individual atoms in a molecule and determination of the relative content of different groups of heteroatoms. ^{13}C NMR spectroscopy allowed the relative content of aliphatic and aromatic carbons to be estimated [11]. These clusters were stitched together to create the initial primary coal macromolecules, and the ^{13}C NMR of the created 2D coal macromolecules was calculated using ACD/C-NMR prediction software (version 10.04). gNMR software (version 5.0.6.0) was then used to compare the calculated NMR spectra with the experimental NMR spectra. The coal macromolecules were continually adjusted until the NMR data of the final macromolecular structure were in general agreement with the experimental NMR data.

3. Results

3.1. Ultimate Analysis and Proximate Analysis Results

The results of ultimate analysis and proximate analysis are shown in Table 1. As can be seen from Table 1, we chose the FK–3 sample for FTIR, XPS and ^{13}C NMR analyses in this study.

Table 1. Property analyses of the coals.

Sample	M_{ad}	A_{ad}	V_{ad}	FC_{ad}	C	H	O	N	S	H/C	O/C	R_o (%)
FK–2	1.12	15.25	34.15	49.48	83.72	5.32	8.83	1.86	0.27	0.76	0.08	0.83
FK–3	1.82	18.63	32.55	47.00	80.46	5.51	12.32	1.71	0	0.82	0.11	0.81
FK–4	1.15	10.11	35.64	53.10	76.14	4.59	17.95	1.32	0	0.72	0.18	0.76

3.2. Molecular Structure Construction

3.2.1. ^{13}C NMR Spectra Analysis

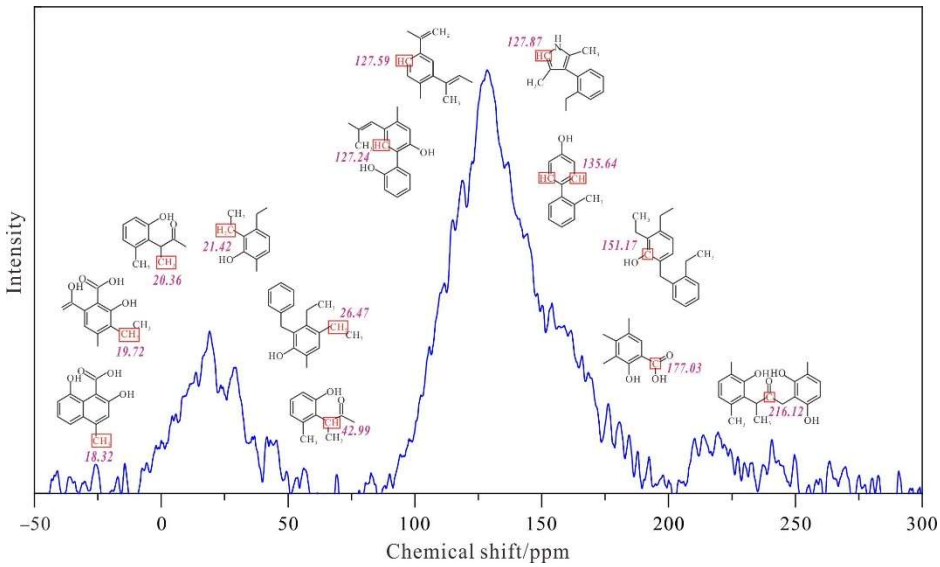

Figure 1. The ^{13}C nuclear magnetic resonance profile of the FK–3 coal with chemical shift assignments. 3.2.2. FTIR Spectra Analysis.

The ^{13}C NMR profiles and chemical shift assignments of the FK–3 coal are shown in Figure 1. Based on the observation that there are four peaks in the NMR spectrum, 18–27 ppm corresponds to aliphatic $–CH_3$, $–RCH_3$ and $–CH_2$, which indicates the presence of some number of aliphatic chains in the coal structure. The prominent peak at 110–150 ppm corresponds to

ISSN: 2710-0588

the chemical shift of aromatic carbon, indicating that aromatic carbon accounts for the most significant proportion of organic carbon in the coal in total. The peak at 150–190 ppm corresponds to carboxyl carbon and that at 210–220 ppm corresponds to carbonyl carbon, indicating the presence of a large number of oxygen atoms in the coal molecule [14], which is consistent with the results of the elemental analysis (15.38% oxygen).

3.2.2. FTIR Spectra Analysis

The FTIR profiles of the Fukang coal are shown in Figure 3. The peaks located at 700–900 cm^{-1}, 1171 cm^{-1}, 1373 cm^{-1}, 1430 cm^{-1}, 1591 cm^{-1}, 1678 cm^{-1}, 2865 cm^{-1}, 2920 cm^{-1} and 3211 cm^{-1} correspond to $(C–H)_{ar}$, C–O, $–CH_3$, $–CH_2$, C=C, C=O, $–CH_2$, $–CH_3$ and –OH, respectively, evidence of the presence of moisture in the coal samples can be found from the peaks present in the 3000–3300 cm^{-1} wave number range, and the relatively consistent information on coal structure obtained in Figure 1 and Figure 2 are a good indication that both experiments have an essential role in reconstructing the molecular structure of coal [9].

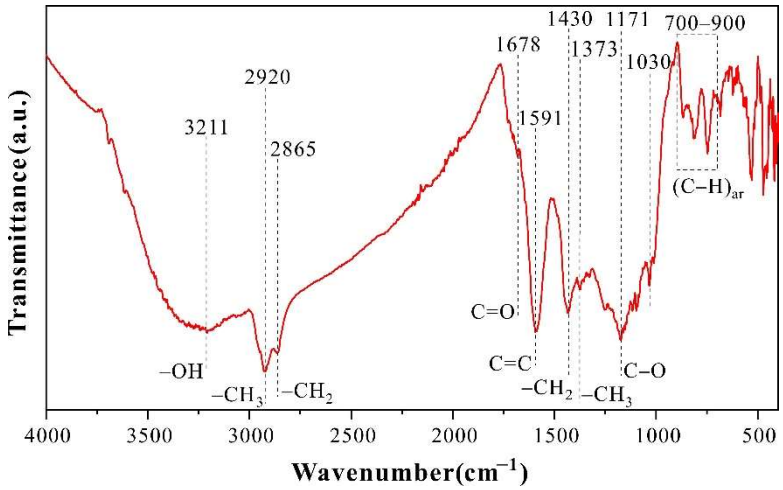

Figure 2. The Fouriertransform interferometric radiometer profile of the FK–3 coal with wavenumber assignments.

3.2.3. Construction and Validation of 2D Coal Molecular Structure

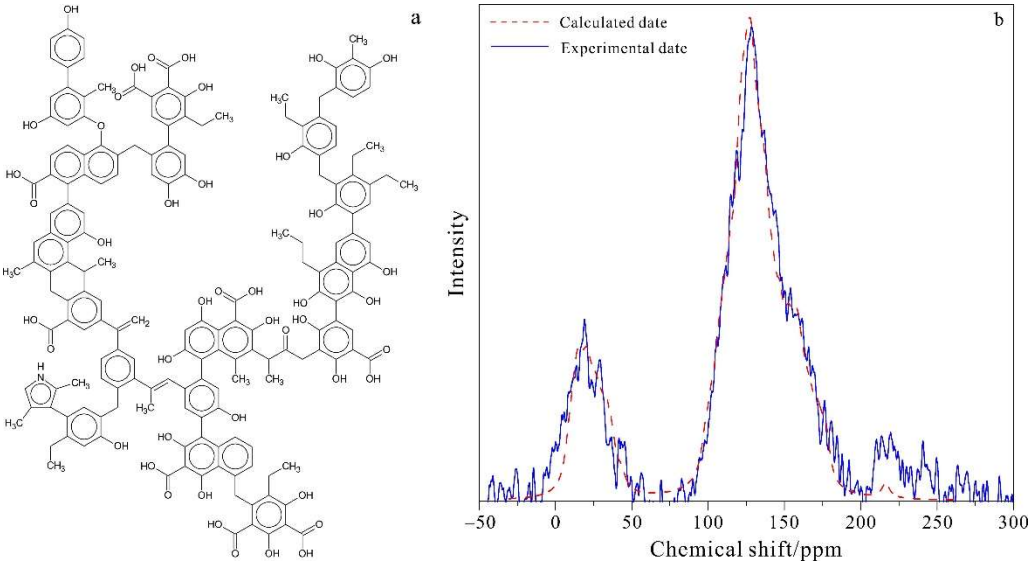

Figure 3. (a) Two-dimensional molecular structure of the FK–3 coal; (b) comparison of experimental data and calculated data.

ISSN: 2710-0588

The 2D chemical molecular structure of Fukang coal was determined according to XPS, FTIR and ^{13}C NMR data, as shown in Figure 3a. Figure 3b compares the ^{13}C NMR data estimated based on the 2D structure and the experimental NMR data. The data obtained from the calculation results agree with the experimental NMR data. The molecular formula of the constructed coal structure is $C_{179}H_{155}NO_{44}$, and the total molecular weight is 3021.

3.2.4. Construction of 3D Coal Molecular Structure

In Figure 4a, the 3D coal structure consists of 14 coal macromolecules with a unit cell size of 3.73 × 3.73 × 3.73 nm and contains 5306 atoms ($C_{2506}H_{2170}N_{14}O_{616}$). In this study, a 1 nm blank slit layer was constructed (Figure 4b) to simulate the adsorption of methane at different temperatures (303.15 K, 323.15 K, 343.15 K and 363.15 K) and pressures (increased from 0.5 to 1.0 to 2.0 to 15.0 MPa). Supercell module was used to construct supercells on the basis of models of methane adsorption at different saturation levels.

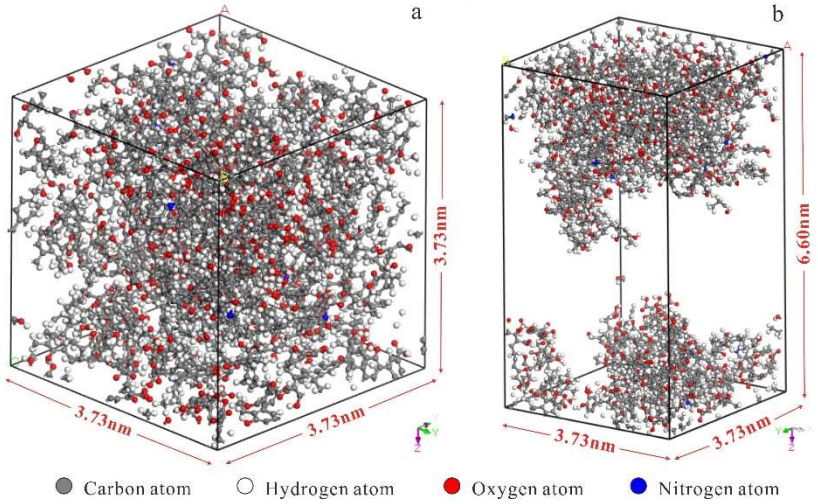

Figure 4. (a) Three-dimensional molecular structure model of the FK–3 coal.; (b) The 3D molecular structure model added with 1 nm blank slit blank layer.

3.2.5. Methane Adsorption Results

When the temperature was 303.15 K, the adsorption capacity of methane increased rapidly when the fugacity was less than 5 MPa and slowly increased when the fugacity was 5–7.83 MPa. When the fugacity was 7.83 MPa, the excess adsorption capacity reached the maximum value of 8.49 mmol/g and reached the saturated adsorption state. When the fugacity was greater than 7.83 MPa, the excess adsorption capacity of methane gradually decreased because, with the increase in fugacity, the kinetic energy of methane molecules also increases, thus decreasing the adsorption on the pore wall and transforming the adsorbed gas into free gas. Under the same fugacity, the excess adsorption capacity decreases with the increase in temperature, and with the increase in temperature, the fugacity required to reach the maximum excess adsorption capacity gradually increases. When the temperature was 323.15 K and the fugacity was 8.09 MPa, the maximum excess adsorption capacity was 7.51 mmol/g. When the temperature was 343.15 K and the fugacity was 11.63 MPa, the maximum excess adsorption capacity was 7.28 mmol/g. However, when the temperature was 363.15 K, the fugacity needed to reach 12.81 MPa to achieve the maximum excess adsorption capacity of 6.81 mmol/g.

3.2.6. Methane Diffusion Results

The diffusion coefficient of methane increased from 2.75×10^{-8} m^2/s to 3.42×10^{-8} m^2/s at a temperature of 303.15 K, an increase in pore size from 1 nm to 4 nm and a pressure of 0.5 MPa, but at a pressure of 15.0 MPa, the diffusion coefficient of methane only increased from 0.38×10^{-8} m^2/s to 0.49×10^{-8} m^2/s, showing that the diffusion coefficient tends to decrease with

ISSN: 2710-0588

increasing pressure. The variation in the diffusion coefficient of methane in coal can be divided into two stages. The first stage is a rapid decrease stage, from 0.5 MPa to 5.0 MPa, where the diffusion coefficient of methane dropped sharply and the diffusion coefficient decreased by 82.89% on average; the second stage is a declining stage, from 5.0 MPa to 15 MPa, where the diffusion coefficient tended to be less but the diffusion coefficient decreased only by 23.74% on average.

4. Conclusion

In this paper, the sorption and diffusion characteristics of methane in Fukang low-rank coal were investigated by molecular simulation. The main results are summarized as follows.

(1) The molecular structure of Fukang coal was characterized by a series of experiments including elemental analysis, FTIR, XPS and ^{13}CNMR. The molecular formula of the constructed 2D coal is $C_{179}H_{155}NO_{44}$. The 3D coal macromolecule structure model consists of 14 coal molecules and its molecular weight is 42294 ($C_{2506}H_{2170}N_{14}O_{616}$).

(2) The excess adsorption of methane shows an increase followed by a decrease with increasing pressure. However, the diffusion of methane shows two phases with increasing pressure: 0.5–5.0 MPa for a sharp decrease in the diffusion coefficient and 5.0–15.0 MPa for a slow decrease in the diffusion coefficient.

(3) The total diffusion energy increases with increasing pressure; however, the total diffusion energy tends to decrease with increasing temperature and pore size. The diffusion activation energy decreases with decreasing pore size.

Acknowledgments

Natural Science Foundation.

References

[1] H.J. Fu, D.Z. Tang, Xu, Tao, et al. Preliminary research on CBM enrichment models of low-rank coal and its geological controls: A case study in the middle of the southern Junggar Basin, NW China. Marine and Petroleum Geology, vol. 83 (2017), 97–110.

[2] H.H. Hou, L.Y. Shao, Yi, Tang, et al. Quantitative characterization of low-rank coal reservoirs in the southern Junggar Basin, NW China: Implications for pore structure evolution around the first coalification jump. Marine and Petroleum Geology, vol. 113 (2020), 104165.

[3] X, Ge, D.M. Liu, Y.D. Cai, et al. Gas Content Evaluation of Coalbed Methane Reservoir in the Fukang Area of Southern Junggar Basin, Northwest China by Multiple Geophysical Logging Methods. Energies, vol. 11 (2018), 1867.

[4] X, Li, X.H. Fu, X.S. Yang, et al. Coalbed methane accumulation and dissipation patterns: A Case study of the Junggar Basin, NW China. Journal of Asian Earth Sciences. vol. 160 (2018), 13–26.

[5] H.J. Fu, D.Z. Tang, H, Xu, et al. Geological characteristics and CBM exploration potential evaluation: A case study in the middle of the southern Junggar Basin, NW China. Journal of Natural Gas Science and Engineering. vol. 30 (2016), 557–570.

[6] J.Q. Kang, X.H. Fu, D. Elsworth, et al. Vertical heterogeneity of permeability and gas content of ultra-high-thickness coalbed methane reservoirs in the southern margin of the Junggar Basin and its influence on gas production. Journal of Natural Gas Science and Engineering. vol. 81 (2020), 103455.

[7] J.Q. Kang, X.H. Fu, L, Gao, et al. Production profile characteristics of large dip angle coal reservoir and its impact on coalbed methane production: A case study on the Fukang west block, southern Junggar Basin, China. Journal of Petroleum Science and Engineering. vol. 171 (2018), 99–114.

ISSN: 2710-0588

[8] J.Q. Kang, X.H. Fu, J, Shen, et al. Characterization of Coal Structure of High-Thickness Coal Reservoir Using Geophysical Logging: A Case Study in Southern Junggar Basin, Xinjiang, Northwest China. Natural Resources Research. vol. 31 (2022), 929–951.

[9] H.J. Fu, D.Z. Tang, T, Xu, et al. Characteristics of pore structure and fractal dimension of low-rank coal: A case study of Lower Jurassic Xishanyao coal in the southern Junggar Basin, NW China. Fuel. vol. 193 (2017), 254–264.

[10] H.J. Fu, D.T. Yan, S.G. Yang, et al. Characteristics of in situ stress and its influence on coalbed methane development: A case study in the eastern part of the southern Junggar Basin, NW China. Energy Science & Engineering. vol. 8 (2019), 515–529.

[11] Y, Li, C, Zhang, D.Z. Tang, et al. Coal pore size distributions controlled by the coalification process: An experimental study of coals from the Junggar, Ordos and Qinshui basins in China. Fuel. vol. 206 (2017), 352–363.

[12] T.F. Jia, S.H. Zhang, S.H. Tang, et al. Characteristics and Evolution of Low-Rank Coal Pore Structure Around the First Coalification Jump: Case Study in Southeastern Junggar Basin. Natural Resources Research. vol. 31 (2022), 2769–2786.

[13] G.Q. Li, D.T. Yan, X.G. Zhuang, et al. Implications of the pore pressure and in situ stress for the coalbed methane exploration in the southern Junggar Basin, China. Engineering geology. vol. 262 (2019), 105305.

[14] H.H. Hou, G.D. Liang, L.Y. Shao, et al. Coalbed methane enrichment model of low-rank coals in multi-coals superimposed regions: A case study in the middle section of southern Junggar Basin. Frontiers of Earth Science. vol. 15 (2021), 256–271.